FACTORS AFFECTING THE INTERFACE APPARENT COEFFICIENT OF FRICTION MOBILISED IN PULLOUT CONDITIONS

N. Moraci
"Mediterranea" University of Reggio Calabria, Italy
G. Romano
"Mediterranea" University of Reggio Calabria, Italy
F. Montanelli
Tenax S.p.A, Viganò Brianza, Italy

ABSTRACT: The paper deals with an experimental research, carried out by means of a new large scale pullout test apparatus, to study the factors affecting the mobilization of the interface interaction mechanisms in pullout loading conditions. More than 40 pullout tests at controlled displacement rate have been performed on different HDPE extruded mono-oriented geogrids embedded in a compacted granular soil varying the reinforcement embedded lengths and the applied vertical effective pressures. The analysis of the test results showed the influence of the several parameters (reinforcement stiffness, geometry and length, vertical effective stress) on the pullout resistance and on the interface apparent coefficient of friction mobilized in pullout conditions. These results can be used, taking into account the long term safety factor, in the design. Moreover, the experimental results clearly showed the effects of dilatancy at the soil–reinforcement interface that occur along the passive failure surfaces, which start at the node embossment and at transversal bars of the geogrid. These effects depend on the soil and geogrid characteristics that influence the dilatancy.

1 INTRODUCTION

In order to analyse the internal stability of reinforced earth structures, it is necessary the evaluation of the reinforcement pullout resistance, mobilized in the portion of reinforcement placed in the anchorage zone.

The pullout resistance (expressed in terms of force per unit width) can be evaluated by using the two following equations:

$$P_R = 2 \cdot L \cdot \sigma'_V \cdot f_b \cdot \tan\phi' \quad (1)$$

$$P_R = 2 \cdot L \cdot \sigma'_V \cdot \mu_{S/GSY} \quad (2)$$

where:

- P_R = Pullout resistance (per unit width);
- L = reinforcement length in the anchorage zone ;
- σ'_V = effective vertical stress;
- ϕ' = soil shear strength angle;
- f_b = soil-geosynthetic pullout interaction coefficient;
- $\mu_{S/GSY}$ = soil-geosynthetic interface apparent coefficient of friction.

The soil-geosynthetic pullout interaction coefficient f_b may be determined by means of theoretical expressions (Jewell et al, 1984, 1985), whose limits have been underlined by different researchers (Palmeira and Milligan, 1989; Wilson-Fahmy and Koerner, 1993; Moraci and Montanelli, 2000; Ghionna et al., 2001), or by the interpretations of pullout tests results by applying the following equation:

$$f_b = \frac{P_R}{2 \cdot L_e \cdot \sigma'_V \cdot \tan\phi'} \quad (3)$$

where:

- L_e = effective reinforcement length

Previous experimental studies (Palmeira and Milligan, 1989; Moraci and Montanelli, 2000; Ghionna et al., 2001), related to pullout tests performed on extruded HDPE geogrids, have shown how the values of f_b, determined by means of the equation (3), are largely influenced by the choice of the value of the soil shear strength angle.

Those studies have shown that the use, in agreement with the conventional design procedures for soil reinforced structures (Jewell, 1991; Jewell, 1996), of the constant volume soil shear strength angle yields, for compacted soils, a lower boundary of the shear strength mobilised in pullout conditions (Moraci and Montanelli, 2000, Moraci et al. 2002).

In absence of a clear indication regarding the choice of the soil shear strength angle to be used for the determination of f_b or of the development of new theoretical expressions that include the evaluation of all the parameters that influence the mobilization of the interaction mechanisms (frictional and passive) in pullout condition, the problem of the determination of the pullout resistance may be overcome by the use of the soil-geosynthetic interface apparent coefficient of friction determined by means of large scale pullout tests, using the following expression:

$$\mu_{S/GSY} = \frac{P_R}{2 \cdot L_e \cdot \sigma'_V} \quad (4)$$

It is important to note that the determination of $\mu_{S/GSY}$ by using equation (4) can be performed without any assumption about the values of the soil shear strength angle mobilized at the interface, since all the parameters of the above equation can be easily determined from the pullout tests.

Anyhow it is important to define the role of all the design (and tests) parameters on the mobilization of the interaction mechanisms (frictional and passive) in pullout condition, including the geosynthetic length, tensile stiffness,

geometry and shape, the vertical effective stress acting at the geosynthetic interface and the soil shear strength.

In the present paper same results of an experimental research carried out in order to study the factors affecting the mobilization of the interface interaction mechanisms in pullout loading conditions are shown.

2 EQUIPMENT AND TEST MATERIALS

The test apparatus is composed by a pullout box (1700x600x680 mm), a vertical load application system, a horizontal force actuator device, a special clamp, and all the required instrumentation, figure 1.

An air filled cushion, in which the air pressure was carefully controlled, applies the vertical load. A steel plate is used to restrain the air cushion on the upper side thus to transfer the load at the soil interface.

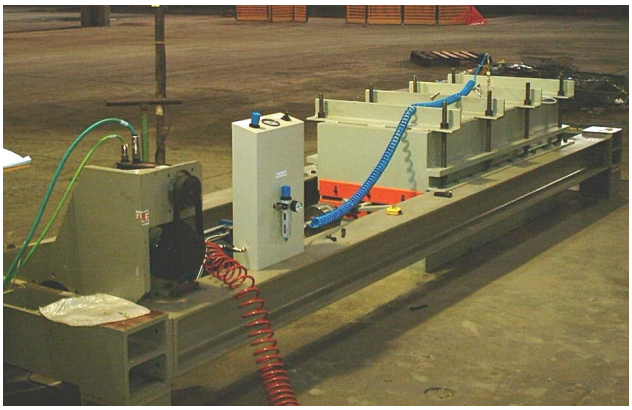

Figure 1 Pullout test apparatus.

An electric jack, as showed in figure 2, applies the pullout force, which is measured using a load cell placed between the electric jack and the clamping system (figure 3).

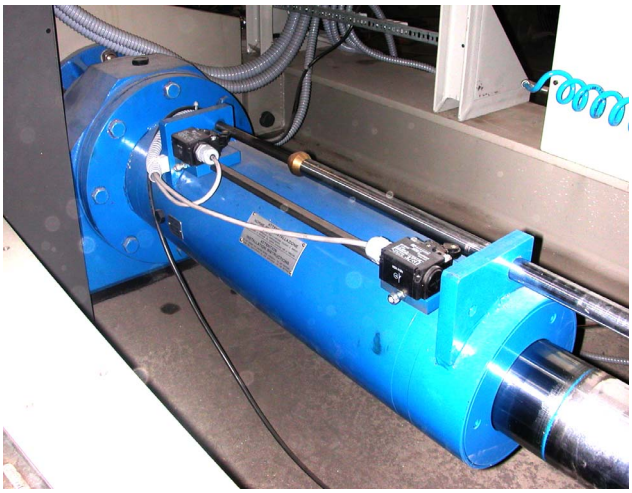

Figure 2 Electric jack.

The apparatus is capable to produce the confined failure of the geosynthetic specimen by using a clamp placed inside the soil, well beyond the sleeve thus to keep the geosynthetic specimen always confined in the soil for the whole test duration.

Friction between the soil and the sidewalls of the box is minimized by use of smooth Teflon sheets.

The equipment incorporates two sleeves (200 mm long) near the slot at the front of the pullout box in order to avoid front wall effects as recommended by a number of researchers (Palmeira and Milligan, 1989; Moraci and Montanelli, 2000; Ghionna et al., 2001).

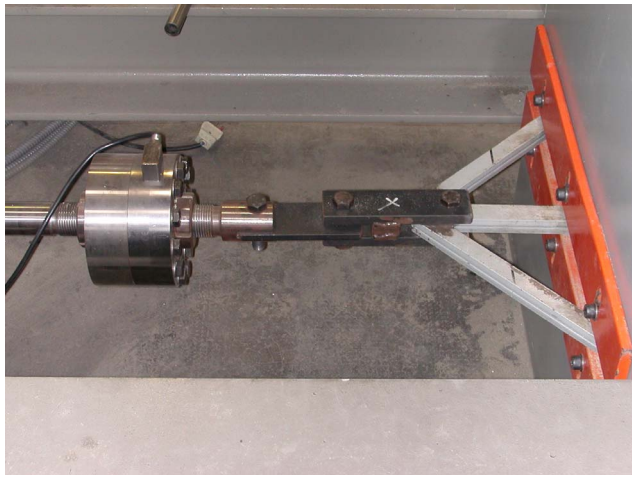

Figure 3 Load cell and clamping system.

The specimen displacements have been measured and recorded through inextensible steel wires connected in at least six different points along to the geogrid specimen. The wire gages were connected to displacements transducers (RVDTs) fixed to the external back side of the box (figure 4).

All the instrumentations are linked to a personal computer that is programmed to scan the measurements at constant time intervals to perform the electronic control and the data acquisition system.

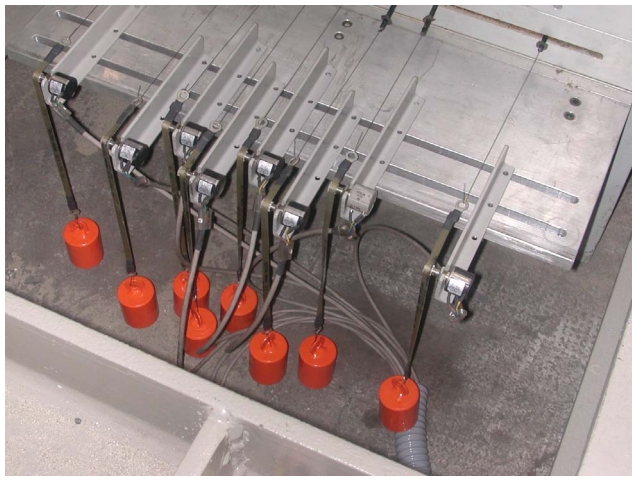

Figure 4 Displacement transducers.

Pullout tests have been performed on three different HDPE extruded mono-oriented geogrids (Tenax TT 090 SAMP, TT 120 SAMP and TT160 SAMP, respectively described as GG1, GG2 and GG3).

The three geogrids show similar geometrical characteristics when analysed in the plain area. They all have the same number of tensile elements per unit width, similar longitudinal rib pitch, and similar elliptical aperture shape.

On the contrary, the three geogrids have different cross sectional shape with main differences in rib and bar thicknesses.

A more detailed analysis of the transversal bar geometry has also shown a non-uniform shape with greater thickness at the rib intersection. At these cross sections and also especially across the transversal bars, the passive in-

teraction mechanisms, that generate the passive component of geogrid pullout resistance, are mobilized.

Therefore, the node and transversal bar geometry has been carefully determined to evaluate the competent passive resistance surfaces. The results of this analysis are reported in table 1, where W_r e B_r are respectively the node width and thickness, W_t e B_t are respectively the width and thickness of the bar portion between two nodes (figure 5), and A_b is the competent area of each rib element (composed of the single node and of the bar portion between two nodes A_t+A_r) where the passive resistance can be mobilized.

Table 1 Structural characteristics of the different geogrids

Geogrid	W_r (mm)	W_t (mm)	B_r (mm)	B_t (mm)	A_b (mm^2)
GG 1	11.26	6.6	3.80	3.57	66.35
GG 2	11.86	6.0	4.65	4.48	85.35
GG 3	12.36	5.5	5.16	4.85	90.45

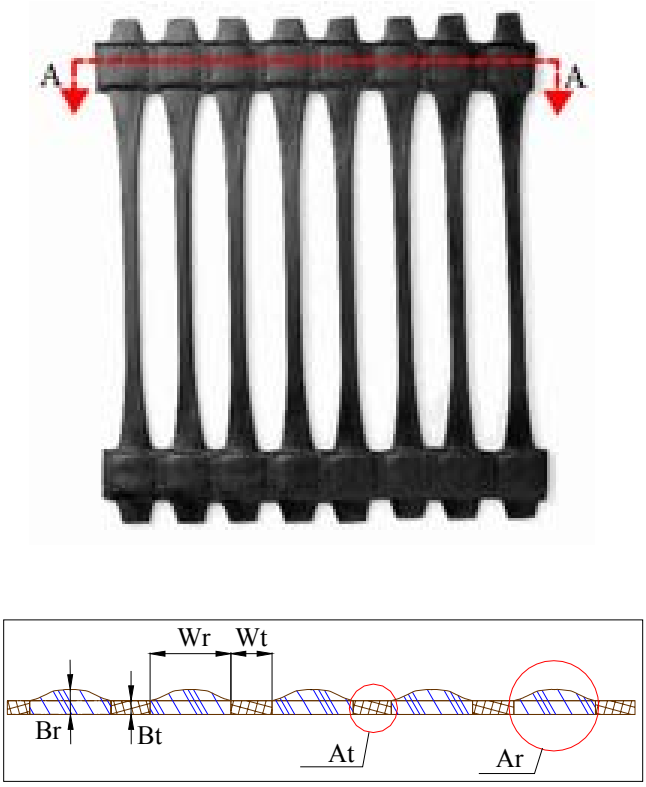

Figure 5 Schematic cross section A-A of the geogrid bar

Wide width tensile tests (EN ISO 10319) on the geogrids have been carried out at different displacement rates of 1 and 100 mm/min. These speeds are respectively the pullout test rate and the wide width tensile test rate.

The tensile test results are reported in Table 2.

Table 2 Wide width tensile moduli at 2% and 5% strain and peak tensile strengths at different displacement rates

Geogrid	Test rate (mm/min)	$J_{2\%}$ (kN/m)	$J_{5\%}$ (kN/m)	T_F (kN/m)
GG1	100	1769.5	1264.4	103.06
GG1	1	946.5	719.5	73.06
GG2	100	2230.0	1687.8	144.36
GG2	1	1338.5	1049.0	98.99
GG3	100	2669.0	1950.2	170.77
GG3	1	1903.0	1354.8	118.29

A granular soil, a medium sand, was used in these tests. The soil was tested for the main geotechnical parameters.

The results of the classification tests indicate that the soil is a uniform medium sand (A-3 according to CNR-UNI 10006 classification system), with uniformity coefficient $U=d_{60}/d_{10}$ =1.5 and average grain size d_{50}=0.22 mm, figure 6.

The Standard Proctor compaction test performed indicates a maximum dry unit weight γ_{dmax}=16.24 kN/m^3 at a water content w_{opt} =13.5%.

Direct shear tests performed at an initial unit weight equal to 95% of γ_{dmax} (obtained at a water content of 9%), yield very high single values of the peak shear strength angle ϕ'_p, in the range between 48° and 42°, where the higher and the lower values refers respectively to the lower (σ'_v=10 kPa) and the higher (σ'_v=100 kPa) vertical effective confining pressures.

The shear strength angle at constant volume ϕ'_{cv} results equal to 34°.

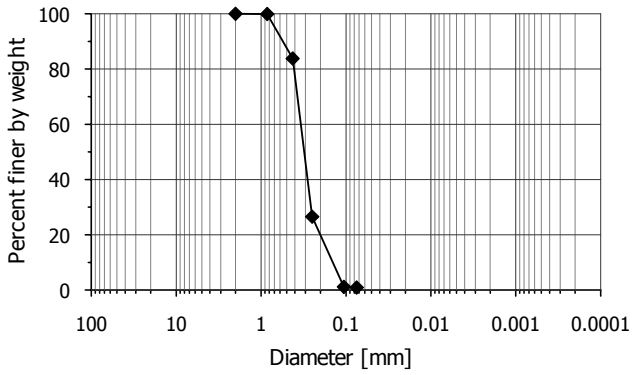

Figure 6 Particle size distribution curve of the soil used in the research.

More than 40 pullout tests have been performed varying the specimen length (L_R= 0.40, 0.90, 1.15 m) while keeping the specimen width constant (B= 0.58 m). Applied vertical effective pressures were equal to 10, 25, 50, 100 kN/m^2. The displacement rate has been equal to 1.0 mm/min for all tests.

For each test condition, the friction between the clamp and the test soil has been evaluated by performing the test without the geogrid. The pullout force values for the clamp alone have been deducted, at each displacement level, from the pullout forces measured in the tests with the geosynthetics at the same displacement.

All tests have been performed until geogrid rupture or till a total horizontal displacement of 100 mm was achieved. For all the tests, the geogrid specimens remained always confined within the soil for its whole length.

3 TEST RESULTS

The test results in terms of pullout resistance (per unit width) are summarized in table 3.

Table 3. Peak pullout resistance, Pr (kN/m), measured during the tests.

Geogrid	Specimen Length (m)	Normal stress σ'v			
		10 kPa	25 kPa	50 kPa	100 KPa
GG1	0.40	9.62	18.44	33.76	39.03
GG1	0.90	16.62	34.55	52.52	78.52*
GG1	1.15	20.00	38.46	53.74	72.50*
GG2	0.40	14.29	24.03	40.80	56.59
GG2	0.90	22.31	39.99	70.07	103.99
GG2	1.15	26.77	51.43	77.63	108.60*
GG3	0.40	10.85	24.76	37.45	58.67
GG3	0.90	19.86	41.80	72.95	101.08
GG3	1.15	24.35	41.4	81.77	115.28

* Specimen failure

Figures 7 to 9 show, for the geogrids GG1, GG2 and GG3, the trend of the pullout interface apparent coefficient of friction $\mu_{S/GSY}$ (evaluated at the peak of pullout resistance) as a function of the vertical effective applied stress. In each figure, the results refer to the three different specimen lengths used.

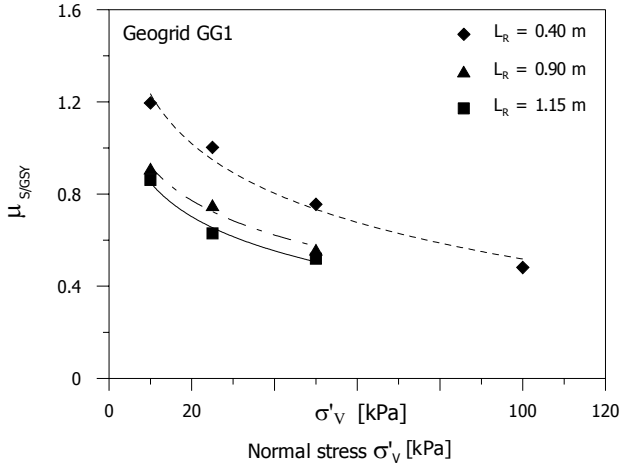

Figure 7 Interface apparent friction coefficient vs. vertical effective stress for geogrid GG1 at different specimen lengths

In all the analysed cases (for different geogrid types and different lengths) it is possible to observe a reduction in the mobilized peak pullout interface apparent friction coefficient with the increase of the applied vertical effective stress. Moreover, it is possible to note that the lower values of $\mu_{S/GSY}$ are given with the longer specimens.

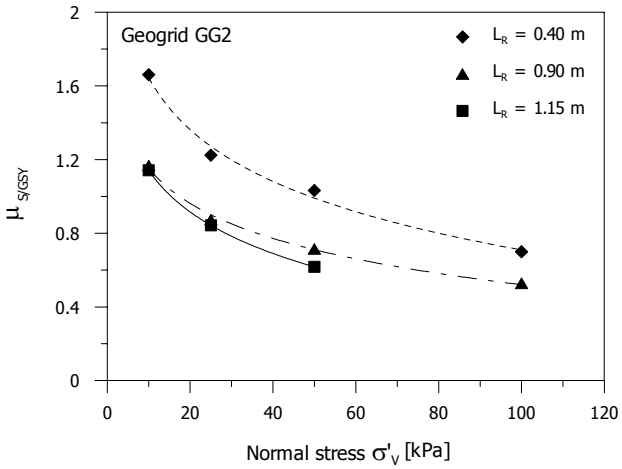

Figure 8 Interface apparent friction coefficient vs. vertical effective stress for geogrid GG2 at different specimen lengths

These results are due to two different phenomena:

- the first, of greater importance, is connected to the soil dilatancy phenomena that develop in correspondence with the three-dimensional passive failure surfaces that arise at the node embossments and at geogrid transversal bars. Due to these phenomena, whose entity decreases with the increases of the confining vertical effective stress, two main effects develop:
  - the first is due to the different work necessary to expand the dilatancy surface at different vertical effective confining stresses (these effects generate, in dense granular soils, the failure envelope curve);
  - the second effect is due to the restriction of the dilatancy connected to the nearby soil stiffness (constrained dilatancy), which yields a local increment of the effective confining stress.
- the second effect, of less intensity, is due to the extensibility of the reinforcement that modifies the interface tangential stress distribution and the corresponding pullout resistance strength.

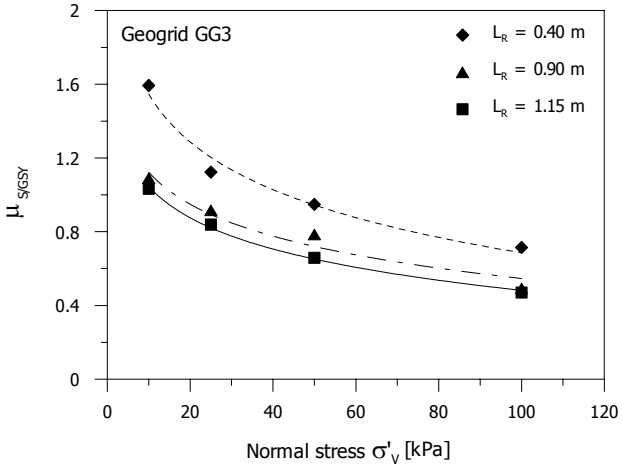

Figure 9 Interface apparent coefficient of friction vs. vertical effective stress for geogrid GG3 at different specimen lengths

By analysing the results, it is noted that the peak mobilized apparent interface friction coefficient for low vertical effective confining stress (10 kPa) is much higher than the corresponding one measured at higher vertical effective stresses (50 o 100 kPa) due the dilatancy behaviour.

Figures 7 to 9 show the percentage variations of the peak mobilized apparent interface coefficient of friction ranging from 148% to 66% for geogrid GG1, from 137% to 85% for geogrid GG2 and from 135% to 120% for geogrid GG3. In particular, the greater percentage increments are for the geogrids having shorter anchorage lengths (L_R= 0.40 m) and the lower increments for the longer anchorage lengths (L_R= 1.15 m).

The reinforcement extensibility effects can be enhanced comparing, for equal vertical effective confinement stress, the apparent interface coefficient of friction values determined for the “long” reinforcement specimens (L_R= 1.15 m) with those evaluated for the “short” ones (L_R= 0.40 m). Figures 7 to 9 show the percentage differences of the peak mobilized apparent interface coefficient of friction due to the reinforcement extensibility that are up to 45% for geogrid GG1, up to 46% for geogrid GG2 and up to 52% for geogrid GG3.

Figures 10 to 12 show the influence of the reinforcement stiffness, and structural characteristics on the mobilized interface apparent coefficient of friction.

In these charts, the interface apparent coefficient of friction is plot as function of the vertical effective confining stress.

The experimental results, interpreted as function of the different longitudinal tensile stiffness, do not show a specific possible regression. In fact, the three geogrids have a progressive tensile stiffness, but the differences in tensile properties cannot be associated to a corresponding difference in pullout resistance.

By comparing the trend of the $\mu_{S/GSY}$ as a function of the applied vertical effective stress, it is possible to notice that the lower values of the apparent coefficient of friction are associated to the geogrid GG1, while the higher values are associated either to the geogrid GG2 or GG3.

Therefore, while there is always an increase of the interface apparent coefficient of friction by passing from the geogrid GG1 to the geogrid GG2 and GG3, the comparison between GG2 and GG3 is less significant with differences in the order of 10%.

Since the geogrid GG2 and GG3 have similar structural characteristics including similar bearing area A_b (competent area of each unit element: composed of the single node and of the half bar portion between two nodes) upon which the passive resistance is mobilized, it is possible to suppose that the values of the soil-geosynthetic interface apparent coefficient of friction $\mu_{S/GSY}$ are mainly influenced by the structural characteristics (geometry and shape) of the geogrids.

In fact, by comparing the experimental results of the tests carried out on the three different geogrids, with the same anchorage lengths and normal stress, in a way not to be influenced by the reinforcement extensibility and by the dilatancy effects, it is possible to observe that the maximum percentage difference of $\mu_{S/GSY}$ is in the order of 20% to 49% with an average value of 34%. These values are very closed to the percentage difference of the competent bearing areas (A_b) between geogrid types (see table 1) upon which the passive resistance is mobilized.

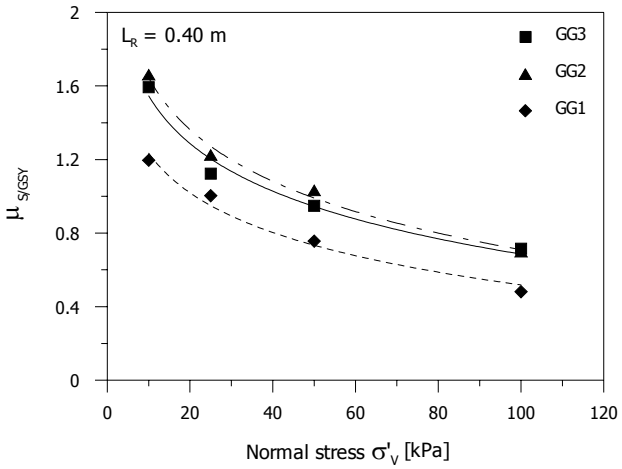

Figure 10 Interface apparent coefficient of friction vs. vertical effective stress for different geogrids at L_R=0.4 m

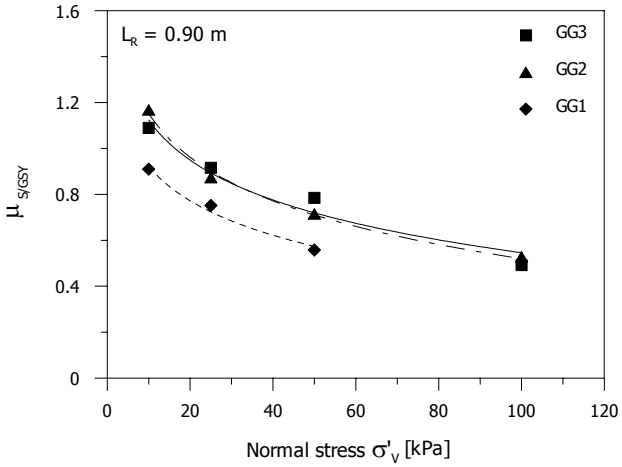

Figure 11 Interface apparent coefficient of friction vs. vertical effective stress for different geogrids at L_R=0.9 m

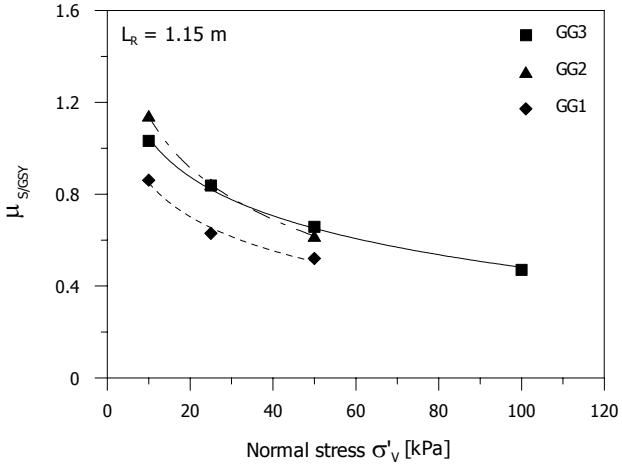

Figure 12 Interface apparent coefficient of friction vs. vertical effective stress for different geogrids at L_R=1.15 m

4 CONCLUSION

The test results clearly show the influence of the different parameters studied (reinforcement stiffness and structure, embedded length and vertical effective stress) on the interface apparent coefficient of friction mobilized in pullout conditions.

- Experimental results clearly show that, due to dilatancy effect, the interface apparent coefficient of friction mobilized at low vertical effective confining pressure (10 kPa) is higher than at high confining pressure (50 or 100 kPa). The dilatancy phenomena develop in correspondence of the passive failure surfaces, which are generated in correspondence of the node embossment and of the geogrid transversal bars. Due to these phenomena, whose entity decreases with the corresponding increase of the vertical effective confining stress, two main effects develop: the first is due to the different work necessary to expand the dilatancy surface at different vertical effective confining stresses (these effects generate in dense granular soils the failure envelope curve); the second effect is due to the restriction of the dilatancy connected to the nearby soil stiffness (constrained dilatancy), that yields a local increment of the effective confining stress. The maximum percentage differences of interface apparent coefficient of friction, due to the dilatancy effects, were observed for the “short” reinforcement layers (L_R= 0.40 m). In this case, the percentage reduction in the mobilized peak pullout interface apparent coefficient of friction with the increase of the applied vertical effective stress ranging between 148% (for geogrid GG1) to 120% (for geogrid GG3); while for the “long” (L_R= 1.15 m) reinforcement layers the maximum percentage variations of $\mu_{S/GSY}$ are ranging between 120% (for geogrid GG3) and 66% (for geogrid GG1).
- The experimental results have shown that the dilatancy effects are predominant in comparison to the effects due to reinforcement extensibility. In fact, at the same normal confining stresses, the values of the interface apparent coefficient of friction evaluated for the “long” reinforcement (L_R = 1.15 m) compared to the values obtained for the “short” reinforcement (L_R = 0.40 m) are ranging between 45% (for geogrid GG1) to 52% (for geogrid GG3).
- The empirical results show an increase in the pullout strength, and therefore of the mobilized interface apparent coefficient of friction, while increasing the competent bearing area of the each node (A_b), upon which the passive mechanism are mobilized. The differences of the values of interface apparent coefficient of friction related to the geogrid structure (shape and geometrical characteristics) are ranging from 20% to 49% with an average value of 34%. These values are very closed to the percentage differences of the competent bearing areas (A_b) between the geogrids upon which the passive resistance is mobilized (ranging from 29% to 37%).
- Test results also show that the influence of reinforcement tensile stiffness on pullout resistance and on interface apparent coefficient of friction ($\mu_{S/GSY}$) is, for the tests conditions, generally negligible.

5 REFERENCE

EN ISO 10319, 1992. Geotextile Wide-Width Tensile Test. International Organization for Standardization, ISO, Ginevra.

Ghionna, V.N., Moraci, N. and Rimoldi, P. 2001. Experimental evaluation of the factors affecting pullout test results on geogrids. Proc. International Symposium: Earth Reinforcement: IS Kyushu 2001, Fukuoka, Japan.

Hayashi, S., Alfaro, M.C., Watanabe, K. 1996. Dilatancy effects of granular soil on the pullout resistance of strip reinforcement. Proc. Earth Reinforcement, Osaka, Japan pp. 39-44. Rotterdam: Balkema.

Jewell, R.A. 1984. Design Methods for Steep Reinforced Embankments. Polymer Grid Reinforcement in Civil Engineering. Thomas Telford, London, pp. 70-81.

Jewell, R.A. 1991. Application of Revised Design Charts for Steep Reinforced Slopes. Geotextiles and Geomembranes, vol.10, n.4, pp. 203-233.

Jewell, R.A. 1996. Soil Reinforcement with geotextiles. Special Publication 123. CIRIA. Thomas Telford, London, pp. 332.

Jewell, R.A., Milligan, G.W.E., Sarsby, R.W. e Dubois, D.D. 1985. Interactions Between Soil and Geogrids. Proc. from the Symp. on Polymer Grid Reinforcement in Civil Engineering. Thomas Telford, pp. 18-30.

Matsui, T., San, K.C., Nabesahima, Y., Amin, U.N. 1996. Bearing mechanism of steel reinforcement in pull-out test. Earth Reinforcement, Ochiai, Yasufuku e Omine, Osaka University, Japan.

Moraci, N. and Montanelli, F. 2000. Analisi di prove di sfilamento di geogriglie estruse installate in terreno granulare compattato. Rivista Italiana di Geotecnica 2000, 4, pp. 5 - 21.

Moraci, N., Romano, G. and Montanelli, F. 2003. Interface pullout behaviour of geogrid embedded in compacted granular soils. XIII European Conference on Soil Mechanics and Geotechnical Engineering, Prague, Vol.1,pp. 837 - 842.

Moraci, N., Romano, G., Gioffrè, D., Montanelli, F. and Rimoldi, P. 2002. Pullout behaviour of geogrid embedded in granular soils. Proc. 7th International Conference on Geosynthetics, Nice, Vol.4,pp. 1345 - 1348.

Palmeira, E.M., Milligan, G.W.E. 1989. Scale and Other Factors Affecting the Results of Pull-out Tests of Grid Buried in Sand. Geotechinique 11, N. 3, 511-524.

Wilson-Fahmy, R.F., Koerner, R.M., 1993. Finite Element Modelling of Soil-Geogrid Interaction with Application to the Behavior of Geogrids in a Pullout Loading Condition. Geotextiles and Geomembranes, n.12, pp.479-501.Ed. Elsevier, London.